Journal of chemical & engineering data

Article

pubs.acs.org/jced

New Series of Green Cyclic Ammonium-Based Room Temperature Ionic Liquids with Alkylphosphite-Containing Anion: Synthesis and Physicochemical Characterization.

Ramzi Zarrougui,*[,†,‡] Noureddine Raouafi,[‡] and Daniel Lemordant[§]

[†]Laboratoire Méthodes et Techniques d'Analyse Institut National de Recherche et d'Analyse Physico-Chimique (INRAP) Pôle Technologique, Sidi Thabet 2020, Tunisia

[‡]Laboratoire de Chimie Analytique et Électrochimie, Faculté des Sciences de Tunis, Université de Tunis El-Manar, Rue Béchir Salem Belkheria, Campus Universitaire de Tunis El-Manar, Tunis El-Manar 2092, Tunisie

[§]Laboratoire de Physicochimie des Matériaux et des Électrolytes pour l'Énergie (PCM2E) EA 6296, Université de F. Rabelais, Faculté des Sciences et Techniques, Parc de Grandmont, 37200 Tours, France

Supporting Information

ABSTRACT: A new series of 12 cyclic ammonium-based room temperature ionic liquids (RTILs) containing an alkylphosphite anion have been synthesized by an alkylation reaction between cyclic tertiary amines and dialkylphosphite. This method constitutes an eco-friendly pathway to RTILs that does not generate any secondary byproducts and avoiding the metathesis reaction involving uses of nonfriendly or expensive salts. Their physicochemical and electrochemical properties have been investigated. The temperature dependency of density, dynamic viscosity, and ionic conductivity were determined at temperatures varying from 293.15 to 323.15 K and were discussed on a structural basis. For the prepared RTILs, the viscosity values are fairly high and low ionic conductivity as compared to usual ILs. The transport properties were found to be temperature-dependent and followed the Arrhenius law. The RTILs potential windows (ΔE) are comprised between 3.00 and 4.77 V. The electrochemical stability seems to be influenced by the alkyl side chain. An increasing in the carbon number of the cation and anion side chain decreases the electrochemical window of RTILs. The correlation between ionic conductivity and viscosity was studied on the basis of the Walden rule, and the new RTILs can be classified as associated ionic liquids (AILs), an intermediate between a true, ionic liquid and a molecular species.

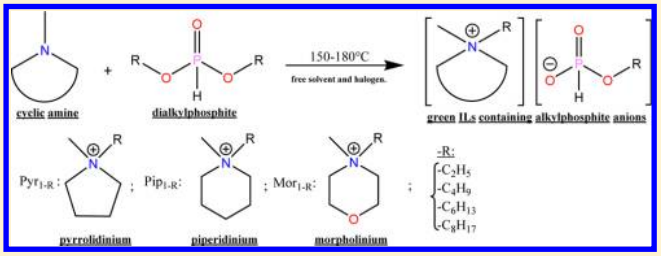

1. INTRODUCTION

During the past decade, RTILs have attracted considerable attention as highly useful solvents and nonaqueous electrolytes because of their many specific and unique physicochemical properties. Indeed, they possess high chemical and thermal stabilities, negligible vapor pressure, high ionic conductivity, and wide potential windows.[1,2] Currently, they are widely studied in many physicochemical and biological fields, including inorganic and organic chemistry, electrochemistry, and catalysis.[3−5] This new brand of solvents has become a novel solution to problems encountered with organic solvents and the limitations met in electrochemical systems.[6,7] The large choice in the existing cations, i.e., imidazolium, tetraalkylammonium, pyrrolidinium, pyridinium, piperidinium, sulfonium, and phosphonium, and in anions ($TFSI^-$ (bis(trifluoromethane sulfonyl)imide), NO_3^-, RCO_2^- and fluorocomplex salts BF_4^-, PF_6^-, AsF_6^-, etc.) in RTILs allows the development of task-specific RTILs for many specific applications such as stereo-selective organic synthesis,[8−10] nanoparticles formation,[11] extraction of toxic metallic cations, and dissolution of biomass.[12,13] However, structural modifications are known to affect RTIL physicochemical properties; therefore, it is of great importance to understand the relationship between structural changes and ILs properties in order to fully deduct and explore their potential applications.

In the past decade, the interest in ionic liquids has been increasing rapidly and especially by the appearance of new ILs with very attractive properties.[14,15] Every year, many new ionic liquids are synthesized.[16−19] There are two basic methods for the preparation of ionic liquids. The aprotic ionic liquids are usually prepared through two successive steps: (1) alkylation of tertiary amine to a quaternary ammonium salt by reaction with an alkyl halide and (2) halide metathesis with a different anion. Protic ionic liquids are synthesized from an acid−base reaction between an organic base like amine and an acid like carboxylic acid. If both are strong enough, proton transfers from the acid to the base occurs.[20,21] Before ILs characterization, a careful control of their purity should be done by determining the level of impurities and additives (water, halides, and cosolvents)

Received: August 11, 2013
Accepted: March 10, 2014
Published: March 19, 2014

remaining in the ILs from the different preparation steps, since they will considerably affect their physical properties.[22]

Recently, many new families of ILs based on tetraalkylammonium, tetraalkylphosphonium, and trialkylsulfonium cations have been reported, and they were obtained in one step by the alkylation of amines, using the alkylphosphates ($[(R-O)_3P=O]$) and alkylsulfates.[23,24] However, information on the synthesis of ILs based on alkylhposphites $[(R-O)_2PH=O]$ anions is relatively limited in the literature.[25] A series of alkylimidazolium ILs containing dialkylphosphate or alkylphosphite anion prepared by a facile, one-pot procedure as RTILs and have the potential to solubilize cellulose under mild conditions.[26] Generally, the ILs with alkylsulfate anions are used in the liquid−liquid extraction of toxic aromatic compounds and sulfur-containing compounds from petroleum products.[27−31]

In this context, we propose in this work the synthesis of 12 new RTILs containing alkylphosphite anions. These ILs were obtained from the alkylation of the ternary cyclic amine (*N*-methylpyrrolidine, *N*-methylpiperidine, and *N*-methylmorpholine) by dialkylphosphite $[(R-O)_2PH(O)]$, with R/C_nH_{2n+1} (n = 2, 4, 6, and 8). The physicochemical characteristics, including their density, dynamic viscosity, ionic conductivity, and electrochemical stability were particularly emphasized.

2. EXPERIMENTAL SECTION

2.1. Chemicals. *N*-Methylpyrrolidine (97%), *N*-methylpiperidine (99%), 4-methylmorpholine (99%), diethylphosphite (99%), dibutyl-phosphite (99%), 1-hexanol (99%), and 1-octanol (99.5%) were purchased from Sigma-Aldrich and freshly distilled before use. Dihexylphosphite and dioctylphosphite were prepared by transesterification of diethylphosphite with the corresponding alcohols according to the literature.[32,33] Diethyl phosphite (69.05 g, 0.50 mol) and 1-hexanol (102.17 g, 1.00 mol) or 1-octanol (130.23 g, 1.00 mol) were introduced in a round-bottom flask connected to a Claisen distillation fitted with a downward condenser and a receiver for vacuum distillation. The resulting solution was heated to 140 °C at 120 mm to 160 mm. Ethanol evolution ceased after about 2 h to 3 h of heating. The remaining crude product was purified by distillation under reduced pressure.

2.2. Synthetic Procedure of Alkyl Phosphite-Containing ILs. The most important feature of diesters of phosphonic acids (referred to them as H-phosphates) is that these compounds exist as an equilibrium mixture of two tautomeric forms of phosphorus(III) and phosphorus(IV) (Scheme 1).

Scheme 1. Tautomeric Equilibrium of Dialkylphosphite

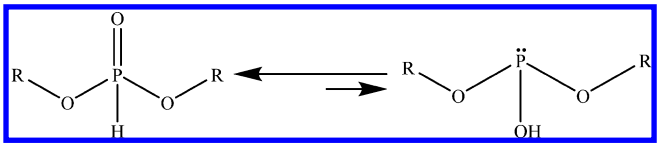

The tautomeric equilibrium of diesters of phosphonic acids is almost totally shifted toward the H-phosphonate forms. Taking into account this fact and the pK_a values of the reactive compounds (approximately 13 for diethylphosphite to >21 for the dicotylphosphite),[32] the acid−base reaction between the amine ($7 < pK_a < 10.5$) and the H-phosphate is practically negligible. This shows the ionic liquid is obtained by the N-alkylation reaction. The RTILs were obtained in one step from the alkylation of cyclic tertiary amine (*N*-methylpyrrolidine, *N*-methylpiperidine, and *N*-methylmorpholine) by the dialkylphosphite $[(R-O)_2PH(O)]$ at a temperature from 150 °C to 180 °C under ambient atmosphere in the absence of solvent as shown in Scheme 2.

Dialkylphosphite and 1.2 mol equiv of the cyclic amine were mixed together at room temperature and heated to reflux at temperature from 150 °C to 180 °C, for 15 h under nitrogen atmosphere under vigorous stirring. After the reaction was complete, the oily mixture was allowed to cool to room temperature and the excess of amine is removed under reduced pressure with a rotary evaporator. The reaction products resulting from diethylphosphite and dibutylphosphite were washed three times with *n*-hexane, and ILs obtained from dihexylphosphite dioctylphosphite were washed with deionized water in order to remove residual amines and unreacted dialkylphosphite. The ionic liquid was extracted twice with ethyl acetate. It was then concentrated by rotary evaporation in vacuum. The slightly yellowish ionic liquids is kept in bottles under an inert gas and were dried at 80 °C under reduced pressure (approximately equal to 20 mmHg) for several days. The yields were superior to 90 % for all synthesized ILs. Before use, the water content of ILs was evaluated by a Karl−Fischer moisture titrator (Metrohm 73KF coulometer), and the values were found lesser than 100 ppm (see Table 2).

2.3. Instrumentation. *2.3.1. Densities Measurements.* The density of all synthesized ionic liquids was determined by using an Anton Parr densitometer (model 60/602, Anton Parr, France). The densitometer was calibrated for the temperatures ranging from 293.15 K to 323.15 K with degassed water and dry air at ambient pressure. Each density measurement was determined four times, and an average value was selected. The estimated uncertainty in density value was less than or equal to $5 \cdot 10^{-5}$ g·cm^{-3}.

2.3.2. Viscosities Measurements. In order to determine the viscosity of the new ILs, TA Instruments rheometer (model AR-1000) with a conical geometry was used. The cell temperature was regulated within ± 0.01 K with a thermostat. The rheometer was calibrated using a Brookfield's viscosity standard (12 700 mPa·s at 298.15 K). The viscosity was determinate for the temperatures ranging from 293.15 K to 323.15 K at the ambient pressure. The uncertainty of measurements is less than ± 1 %.

2.3.3. Conductivities Measurements. A conductivity cell with platinum electrode (Philips PM-6303) was used to determine the ionic conductivity of the selected ILs. The area of platinum electrodes is about 0.25 cm^2, and the distance between two platinum electrodes is about 0.50 cm. The cell constant (K) is 1.061 cm^{-1}, determined by the KCl standard solution. The temperature in the cell was regulated within ± 0.01 K with a thermostat bath. The conductivities values were initially determined as a function of the temperature during a heating cycle from 293.15 K to 323.15 K. Then, the cell was cooled to 288.15 K and after a short time, the measurements were taken. The uncertainty of measurements is less than ± 2 %.

2.3.4. Electrochemical Measurements. Cyclic voltammetry (CV) and linear sweep voltammetry (LSV) measurements were carried out in a conventional three-electrode cell connected to a potentiostat (Radiometer Voltalab PGZ10). The working electrode was a glassy carbon (GC; 1.0 mm in diameter), the counter electrode was a platinum (Pt; 1.6 mm diameter), and the reference electrode was Ag/AgCl, KClsat$_{(PIL)}$. The

dx.doi.org/10.1021/je4007053 | J. Chem. Eng. Data 2014, 59, 1193−1201

Scheme 2. Schematic Reaction of the ILs Preparation[a]

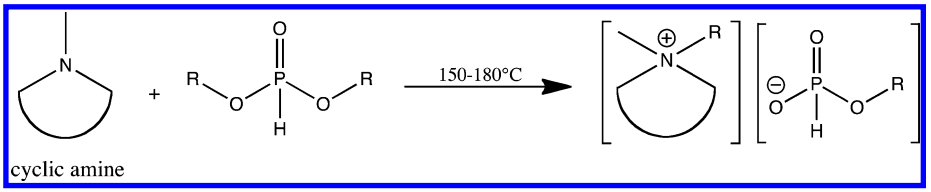

[a]···R = ···C_2H_5, *n*···C_4H_9, *n*···C_6H_{13}, and *n*···C_8H_{17}.

reference Ag/AgCl, KClsat$_{(PIL)}$ is calibrated versus the SHE electrode using the ferrocenium/ferrocene couple. Before each voltammetry study, the electrodes were cleaned using a nitric acid solution and an ultrasound bath to remove any deposited absorbent on the active surface. All measurements were performed in an inert gas atmosphere.

3. RESULTS AND DISCUSSION

3.1. ^{1}H NMR of RTILs. The structure and abbreviation of the RTILs prepared in the present work are reported in Table 1. The structures identification and purity of ILs were confirmed by 400-MHz proton NMR. (Chemical shifts were reported downfield in parts per million (ppm, δ) using tetramethylsilane as internal reference.) The characterization data are as follows.

Table 1. Structures and Abbreviations of RTILs Synthesized in This Work[a]

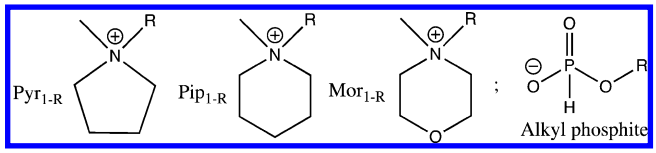

−R	$Pyr_{1\text{-}R}^+$	$Pip_{1\text{-}R}^+$	$Mor_{1\text{-}R}^+$	$anion^{-a}$
$-C_2H_5$	Pyr_{12}^+	Pip_{12}^+	Mor_{12}^+	EP^-
$-C_4H_9$	Pyr_{14}^+	Pip_{14}^+	Mor_{14}^+	BP^-
$-C_6H_{13}$	Pyr_{16}^+	Pip_{16}^+	Mor_{16}^+	HP^-
$-C_8H_{17}$	Pyr_{18}^+	Pip_{18}^+	Mor_{18}^+	OP^-

[a]Pyr, pyrrolidium; Pip, pipiridinium; and Mor, morpholinium. EP^-, ethylphosphite; BP^-, buthylphosphite; HP^-, hexylphosphite; and OP^-, octylphosphite.

N-Ethyl-*N*-methylpyrrolidinium ethylphosphite: ^{1}H NMR (DMSO-d_6) δ (ppm): 3.60 (q, 2H); 3.26 (qw, 2H); 3.3 (s, 3H); 3.24 (t, 2H); 1.68 (m, 2H); 1.22 (t, 3H) 1.17; (t, 3H); and 6.68 (d, 1H).

N-Butyl-*N*-methylpyrrolidinium butylphosphite: ^{1}H NMR (DMSO-d_6) δ (ppm): 0.98 (t, 3H); 1.96 (m, 2H); 1.79 (m, 2H); 3.22 (t, 2H); 3.31 (s, 3H); 1.81 (m, 2H); 1.58 (m, 2H); 0.95 (t, 3H); and 1.43 (m, 2H).

N-hexyl-*N*-methylpyrrolidinium hexylphosphite: ^{1}H NMR (DMSO-d_6) δ (ppm): 0.88 (t, 3H); 1.28 (m, 2H); 1.29 (m, 2H); 1.72 (q, 2H); 3.21 (t, 2H); 3.30 (s, 3H); 3.57 (t, 3H); 1.52 (m, 2H); 1.43 (m, 2H); 1.37 (m, 2H); and 0.87 (t, 3H).

N-Octyl-*N*-methylpyrrolidinium octylphosphite: ^{1}H NMR (DMSO-d_6) δ (ppm): 0.87 (t, 3H); 1.26 (m, 2H); 1.29 (m, 2H); 1.71 (q, 2H); 3.22 (t, 2H); 3.30 (s, 3H); 3.22 (m, 2H); 3.56 (m, 2H); 1.52 (m, 2H); 1.41 (m, 2H); 1.31 (m, 2H); 1.26 (m, 2H); and 0.88 (t, 3H).

N-Ethyl-*N*-methylpiperidinium ethylphosphite: ^{1}H NMR (DMSO-d_6) δ (ppm): 1.25 (t, 3H); 3.28 (q, 2H); 3.21 (m, 2H); 1.74 (m, 2H); 1.60 (m, 2H); 4.02 (q, 2H); and 1.20 (t, 3H).

N-Butyl-*N*-methylpiperidinium butylphosphite: ^{1}H NMR (DMSO-d_6) δ (ppm): 0.89 (t, 3H); 1.3 (m, 2H); 1.71 (m, 2H); 3.22 (t, 2H); 3.20 (m, 2H);1.71 (m, 2H); 1.6 (m, 2H); 3.56 (t, 2H); 1.56 (m, 2H); 1.43 (m, 2H); and 0.93 (t, 3H).

N-Hexyl-*N*-methylpiperidinium hexylphosphite: ^{1}H NMR (DMSO-d_6) δ (ppm): 0.85 (t, 3H); 1.23 (m, 2H); 1.25 (m, 2H); 1.68 (q, 2H); 3.19 (t, 2H); 3.25 (s, 3H); 1.57 (m, 2H); 3.52 (m, 2H); 1.48 (m, 2H); 1.39 (m, 2H); 1.35 (m, 2H); and 0.84 (t, 3H).

N-Octyl-*N*-methylpiperidinium octylphosphite: ^{1}H NMR (DMSO-d_6) δ (ppm): 0.95 (t, 3H); 1.37 (m, 2H); 1.30 (m, 2H); 1.29 (q, 2H); 1.76 (q, 2H); 3.25 (t, 2H); 1.71 (m, 2H);

Table 2. Density, Molar Volume, Isobaric Expansion Coefficient, Viscosity, Specific, Equivalent Ionic Conductivity Electrochemical Windows, and Water Content of RTILs at 298.15 K[a]

ILs	ρ/(g·cm^{-3})	V_m/(cm^3·mol^{-1})	$\alpha_p\cdot10^4$/(K^{-1})	κ/(mS·cm^{-1})	Λ/(mS·cm^2·mol^{-1})	η/(mPa·s)	ΔE/(volt)	water content (ppm)
Pyr_{1-2}-EP	1.12305	198.56	7.05	2.34	464.63	220.1	4.77	21.45
Pyr_{1-4}-BP	1.08159	257.95	6.59	0.27	69.64	321.4	4.07	24.78
Pyr_{1-6}-HP	1.06070	315.83	5.84	0.37	116.85	342.8	3.86	73.97
Pyr_{1-8}-OP	0.98910	395.31	5.39	0.34	134.40	57.85	3.13	16.78
Mor_{1-2}-EP	1.16161	205.74	7.19	0.86	176.93	162.2	4.01	82.25
Mor_{1-4}-BP	1.08158	272.75	6.32	0.77	210.01	217.8	3.40	95.21
Mor_{1-6}-HP	1.01310	346.46	6.04	0.18	62.36	213.3	3.24	51.28
Mor_{1-8}-OP	0.97810	416.11	5.39	0.17	70.73	83.67	2.79	40.08
Pip_{1-2}-EP	1.09413	216.61	7.10	0.72	155.95	91.99	4.95	20.45
Pip_{1-4}-BP	1.05361	278.09	6.51	0.30	83.42	113.3	3.51	55.86
Pip_{1-6}-HP	1.02000	342.15	6.21	0.39	133.43	268.9	3.46	62.46
Pip_{1-8}-OP	0.96940	417.78	5.39	0.33	137.86	37.65	3.26	33.75

[a]Standard uncertainties u are $u(T)$ = 0.01 K, and the combined extended uncertainty U_c is $U_c(\rho) = 5\times10^{-5}$g·cm^{-3}, $U_c(V_m) = 0.01\cdot V_m$, $U_c(\alpha_p) = 0.01\cdot\alpha_p$, $U_c(\kappa) = 0.02\cdot\kappa$, $U_c(\Lambda) = 0.02\cdot\Lambda$, $U_c(\eta) = 0.01\cdot\eta$, and $U_c(\Delta E) = 0.01\cdot\Delta E$ (0.95 level of confidence).

dx.doi.org/10.1021/je4007053 | J. Chem. Eng. Data 2014, 59, 1193−1201

1.60 (m, 2H); 3.46 (m, 2H); 1.54 (m, 2H); 1.43 (m, 2H); 1.30 (m, 2H); 1.28 (m, 2H); and 0.91 (t, 3H).

N-Ethyl-*N*-methylmorpholinium ethylphosphite: ^{1}H NMR (DMSO-d_6) δ (ppm): 1.26 (t, 3H); 3.28 (q, 2H); 3.41 (m, 2H); 3.84 (m, 2H); 4.00 (m, 2H); and 1.21 (t, 3H).

N-Butyl-*N*-methylmorpholinium butylphosphite: ^{1}H NMR (DMSO-d_6) δ (ppm): 0.88 (t, 3H); 1.31 (m, 2H); 1.72 (m, 2H); 3.24 (t, 2H); 3.40 (m, 2H); 3.78 (m, 2H); 3.56 (t, 2H); 1.58 (m, 2H); 1.43 (m, 2H); and 0.95 (t, 3H).

N-Hexyl-*N*-methylmorpholinium hexylphosphite: ^{1}H NMR (DMSO-d_6) δ (ppm): 0.88 (t, 3H); 1.28 (m, 2H); 1.29 (m, 2H); 1.71 (q, 2H); 3.19 (t, 2H); 3.41 (t, 3H); 3.82 (m, 2H); 3.58 (t, 2H); 1.52 (m, 2H); 1.44 (m, 2H); 1.37 (m, 2H); and 0.88 (t, 3H).

N-Octyl-*N*-methylmorpholinium octylphosphite: ^{1}H NMR (DMSO-d_6) δ (ppm): 0.98 (t, 3H); 1.26 (m, 2H); 1.29 (m, 2H); 1.71 (m, 2H); 3.23 (t, 2H); 3.45 (t, 2H); 3.88 (m, 2H); 3.36 (s, 3H); 3.60 (t, 2H); 1.52 (m, 2H); 1.44 (m, 2H); 1.29 (m, 2H); 1.26 (m, 2H); and 0.89 (t, 3H).

3.2. Physical and Chemical Properties of Alkylphosphite-Based RTILs. Several advantages distinguished these new ionic liquids from the usual RTILs. Indeed, these ILs are synthesized in one step using cheap starting chemicals, and the yields of reaction were also high. The counterions to the ammonium cations are alkylphosphates which are not easily oxidizable and thus expending the anodic branch of the electrochemical window. The estimated purities of the synthesized ionic liquids are also high, in the absence of organic solvents and halide ions contaminating the ILs, which would result from using halogenoalkanes and solvents employed for the halide metathesis. Alkylphosphosphite are nontoxic and are usually recommended as a substituent while the alkylating agents used, such as dialkylsulfates, are extremely carcinogenic and renders the reaction inherently hazardous.[34] This would probably make a good candidate for use in in vivo related applications. The experimental physical properties of the RTILs are summarized in Table 2.

3.2.1. Densities and Isobaric Thermal Expansivities. The measured densities of the selected ILs at the temperatures ranging from 293.15 K to 323.15 K at ambient pressure are given in Table S_1 (see the Supporting Information). The ILs densities are comprised between 0.96 g·cm^{-3} and 1.16 g·cm^{-3}. The morpholinium- and pyrrolidinium-based ILs has higher densities than those derived from piperidinium. The density was found to follow in order [$Mor_{1\text{-}n}^+$] > [$Pyr_{1\text{-}n}^+$] > [$Pip_{1\text{-}n}^+$] (n = 2,4) and [$Pyr_{1\text{-}n}^+$] > [$Mor_{1\text{-}n}^+$] > [$Pip_{1\text{-}n}^+$] (n = 6, 8). The molar volume (V_m) calculated from the molecular weight and density of the RTILs at 298.15 K is also shown in Table 2. The molar volume ranges from 198.56 cm^3·mol^{-1} to 417.78 cm^3·mol^{-1}. For a third class of the ring, an increase in the formula weight with increasing number of carbon atoms in the alkyl chain and a decrease in the density causes a subsequent decrease in the molar volume. For the same anion, the molar volume appears to be independent of the nature of the ring. However, for the same cation, the different anions lead to different molar volumes, and the molar volume variations approximately follow the increasing order of the molecular weight of the anions. It is worth noticing that these values are slightly higher than molar volumes of usual ionic liquids.[35] Indeed, the large size of the counterions creating voids between molecules and thus less packing and lower densities. Consequently, this leads to increases in the molar volumes of the RTILs. In Figure 1, we showed the temperature dependence of density for all of the ILs. Density of all ILs vary linearly with the temperature. Using experimental density measurements, the isobaric thermal expansion coefficient α_p of RTILs were calculated using the usual equation:

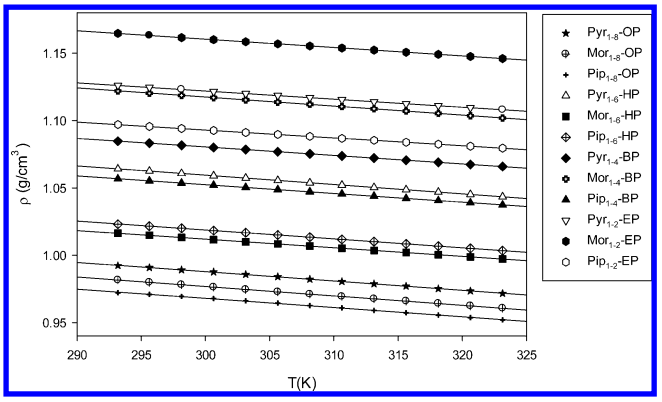

Figure 1. Density of all pyrrolidinium, morpholinium, and piperidinium based ionic liquids as a function of temperature.

$$\alpha_p = -\left(\frac{\partial \ln \rho}{\partial T}\right)_P$$

where ρ is the density in g·cm^{-3}, T is the temperature in K, and P is a fixed pressure. The α_p values for the RTILs are presented in Table 2. The obtained α_p values are of the same order of magnitude of the usual RTILs such as ammonium, imidazolium, and phosphonium-based ones.[36−38] For the same cyclic ammonium, the α_p coefficient decreases following the alkylphosphite anion side chain length increase.

3.2.2. Transport Properties. For an ionic liquid, the viscosity is an essential parameter in analytical and electrochemical studies due to its strong effect on the rate of mass transport and the conductivity within the electrolytic solution. Consequently, the dynamic viscosity of the RTILs have been measured at different temperatures. The experimental data are presented in Table S_2 of the Supporting Information. Commonly, RTILs are more viscous than molecular organic solvents. In fact, their viscosities typically range from 20 mPa·s to approximately 200 mPa·s, but in our case, the values were found to be slightly higher than most of the usual ILs. For instance, at 298.15 K, the viscosities range from 37.6 mPa·s to 321.4 mPa·s. For the same anion, the ionic liquids viscosities are dependent on the nature of the cation. Moreover, for the same alkylphosphite counterion, the dynamic viscosity rises from [$Pyr_{1\text{-}n}^+$]; [$Mor_{1\text{-}n}^+$] to [$Pip_{1\text{-}n}^+$] (n = 2, 4, 6, and 8). However, for similar cations with the same side chain, viscosity differences are due to van der Waals interactions, eventual hydrogen bonds, and electrostatic interactions between the ammoniums and anion species.[39,40] Generally, the dynamic viscosity decreases by 30 % to 60 %, when the cation is pyrrolidinium, morpholinium, and piperidinium, respectively. The viscosity appears to decrease with the ring size and/or the presence of oxygen. A plausible explanation relies on the decrease of the aliphatic van der Waals interactions between cyclic ammonium and alkylphosphite (AP): [$Pyr_{1\text{-}n}$-AP] > [$Mor_{1\text{-}n}$-AP] > [$Pip_{1\text{-}n}$-AP]. Overall, the viscosity increases with increasing chain length of anion: [EP^-] < [BP^-] < [HP^-]. The increase of viscosity is attributed to the strong van der Waals interactions imposed by the increase of the alkyl chain length of anion. The octhylphosphite-based ILs exhibits very lower viscosity than the other ionic liquids ([Pyr_{1-8}-OP]: η = 83.67 mPa·s; [Mor_{1-8}-OP]: η = 57.85 mPa·s

dx.doi.org/10.1021/je4007053 | J. Chem. Eng. Data 2014, 59, 1193−1201

and [Pip_{1-8}-OP]: η = 37.65 mPa·s at 298.15 K. A possible explanation relies on the large size of asymmetrical cyclic ammonium and octylphosphite compared to the other ILs, which weakened considerably the van der Waals interactions between the anion and the cations. Figure 2 shows the

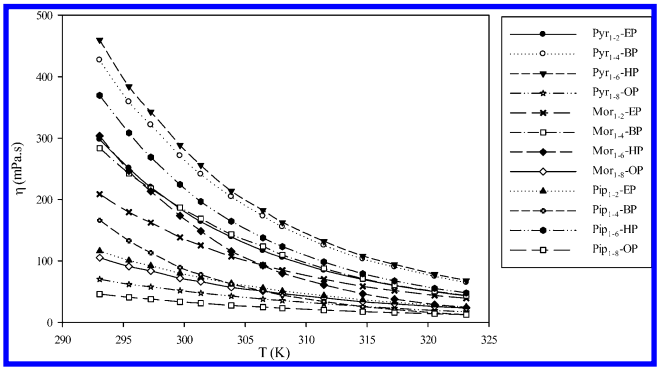

Figure 2. Dynamic viscosity as a function of temperature for the ionic liquids.

temperature dependence of viscosity data for selected ionic liquids. Overall, the viscosity of RTILs decreases drastically by almost 80%, when the temperature increases by 30 °C. This shows the significant effect of the increases in the kinetic energy of ionic species due to the rise in the fluidity in the intermolecular interactions of these ionic liquids.[41] Indeed, the viscosity behavior of the ILs can be understood from the interplay of van der Waals and Coulombic interactions as well as hydrogen bond formation.

The above results show that these nonaqueous electrolytes could be attractive candidates for high temperature applications such as thermal transfer fluids and for reactions needing high boiling and stable solvents. The temperature effect on the ILs viscosity is usually described by the Arrhenius law using Andrade (eq 1).[42]

$$\eta = \eta_\infty \exp\left[\frac{E_{a,\eta}}{RT}\right] \quad (1)$$

where η_∞ is a constant for a given liquid, $E_{a,\eta}$ is the activation energy for the viscous flow, R is the gas constant, and T is the absolute temperature. On the basis of the Andrade equation, the ILs viscosity were found to have an Arrhenius behavior and fits very well to eq 1 for all temperatures. The results gathered on given in Figure 3 show a linear behavior of the logarithmic

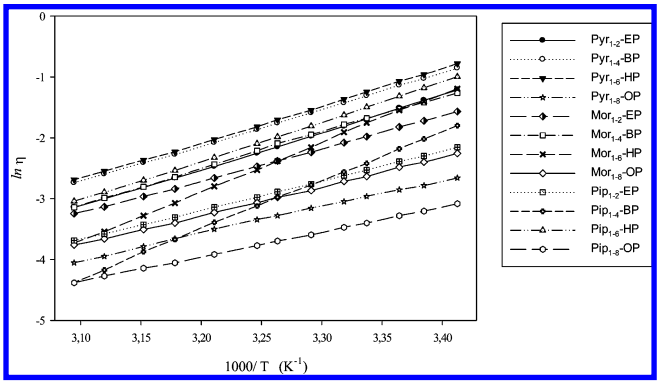

Figure 3. Plot of ln η against 1000/T of the all ILs from the temperature range 293.15 K to 323.15 K.

variation of the viscosity versus 1000/T. Also, the activation energy values for the viscous flow $E_{a,\eta}$ have been extracted from the line slopes. The activation energies $E_{a,\eta}$ and η_∞ values are summarized in Table 3.

The ionic conductivity is one of the most important physicochemical properties of ionic liquids, and they are considered to be used as supporting electrolytes in electrochemical devices. The ionic conductivity of an IL should be related to its viscosity η, the radii of its cation and anion (r_c and r_a), molar volume V_m, as described by eq 2, in which F is the Faraday constant, α_d is the degree of dissociation, ζ_a and ζ_c are the anion and cation microviscosity factors, respectively.[43]

$$\kappa = \frac{\alpha_d F^2}{6\pi N_A V_m \eta}\left[\frac{1}{\xi_a r_a} + \frac{1}{\xi_c r_c}\right] \quad (2)$$

The temperature dependence of conductivity for these ILs are, respectively, shown in Figure 4 and its corresponding experimental data are given in Table S_3 in the Supporting Information. Comparatively, it can be observed that alkylphosphite-based RTILs have lower conductivities then usual ILs.[44,45] The ionic conductivity was found to be less than 1 mS·cm^{-1} except Pyr_{12}-EP (κ = 2.34 mS cm^{-1} at 298.15 K). According to eq 2 and the data in Table 3, the high viscosities, molar volumes, and the radii of nonsymmetric cations and anions of most of the ionic liquids are much involved in considerably value of the electrolyte ionic conductivity. The empirical Arrhenius relation for conductivity is usually used to describe the ion conduction ILs behavior:[42]

$$\kappa = \kappa_0 \exp\left[\frac{-E_{a,\kappa}}{RT}\right] \quad (3)$$

where $E_{a,\kappa}$ is the activation energy for conductivity and κ_0 is the pre-exponential factor. A good fitting of the experimental results is achieved using the Arrhenius model (eq 3) as revealed in Figure 5. The correlated parameters (κ_0 and $E_{a,\kappa}$) determined from the experimental data are presented in Table 3. Moreover, in order to clarify the transport properties (η and κ) relationship and to assess the RTILs ionicity, the Walden plot should be studied.

The Walden rule relates the equivalent conductivity Λ to the fluidity η^{-1} of the medium.[44,46] In this context, the relationship between equivalent conductivity Λ and viscosity η is described by

$$\Lambda \cdot \eta^{\alpha} = \text{const} \quad (4)$$

where α is a positive constant less than or equal to one. The Walden plots in Figure 6 show the variations of ln(Λ) vs ln(η^{-1}) for all selected ILs. The ideal line is generated from data obtained in aqueous 0.01 M KCl solution. We can also determine almost identical values of α from ratio of the activation energies of the transport properties, ($E_{a,\eta}/E_{a,\kappa}$).[47] The fitted α values of the ILs calculated from the slopes of the Walden plots in Figure 6 with those calculated from the activation energies are given in Table 3. According to the rule, if the curves are significantly above the ideal KCl line, then this implies an even faster transport of ions in consideration of the incomplete decoupling of ions in ionic liquids. In this case, the compound is classified as a "good ionic liquid". However, all compounds that lie below 1 order of magnitude of the ideal behavior of diluted KCl solution must be classified as "poor ionic liquids", indicating that the conductivity is lower than

dx.doi.org/10.1021/je4007053 | J. Chem. Eng. Data 2014, 59, 1193−1201

Table 3. Arrhenius Equation Parameters for Viscosity (η_∞ and $E_{a,\eta}$) and Ionic Conductivity (κ_0 and $E_{a,\kappa}$) (Equations 1 and 3 in the Text)[a]

ILs	$\eta_\infty \cdot 10^{10}$ /mPa·s	$E_{a,\eta} \pm \sigma$ /J·mol^{-1}	R^2	κ_0 /mS·cm^{-1}	$E_{a,\kappa} \pm \sigma$ /J·mol^{-1}	R^2	α	α_{AE}
Pyr_{1-2}-EP	2.72	50.6 ± 0.7	0.9996	17.31	22.0 ± 0.6	0.9999	0.42	0.43
Mor_{1-2}-EP	6.33	49.5 ± 0.9	0.9997	118.42	32.1 ± 0.9	1.0000	0.64	0.65
Pip_{1-2}-EP	5.18	50.1 ± 0.8	0.9994	0.20	15.5 ± 0.9	0.9997	0.31	0.31
Pyr_{1-4}-BP	221	36.5 ± 0.5	0.9985	0.20	15.7 ± 0.3	0.9988	0.43	0.43
Mor_{1-4}-BP	26.70	44.2 ± 0.6	0.9996	2.50	19.5 ± 0.7	0.9999	0.42	0.44
Pip_{1-4}-BP	4.11	49.6 ± 0.6	0.9992	0.82	17.1 ± 0.8	0.9995	0.34	0.34
Pyr_{1-6}-HP	0.003	67.2 ± 0.4	0.9997	3.68	24.6 ± 0.9	1.0000	0.36	0.37
Mor_{1-6}-HP	90.30	39.6 ± 0.4	0.9993	0.74	20.6 ± 0.5	0.9996	0.53	0.52
Pip_{1-6}-HP	76.00	40.2 ± 0.6	0.9997	5.02	21.7 ± 0.6	1.0000	0.52	0.54
Pyr_{1-8}-OP	0.002	66.9 ± 0.3	0.9996	31.22	28.5 ± 0.2	0.9999	0.41	0.43
Mor_{1-8}-OP	0.95	53.7 ± 0.3	0.9997	0.42	17.1 ± 0.1	1.0000	0.31	0.32
Pip_{1-8}-OP	428	33.8 ± 0.4	0.9997	0.06	12.9 ± 0.8	1.0000	0.38	0.38

[a] R^2 is the correlated coefficient and σ the standard deviation. α is calculated from the Walden plots (eq 4) and α_{AE} is calculated from the ratio of the activation energies.

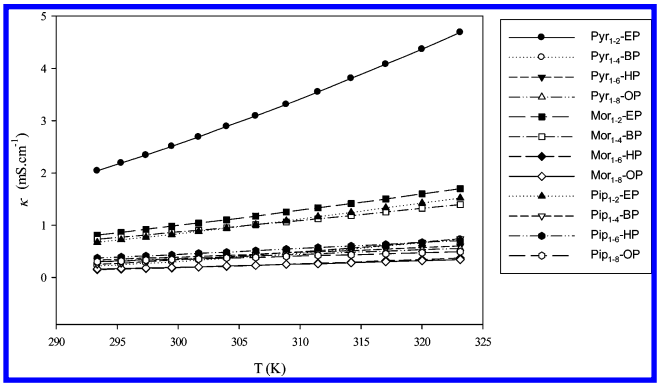

Figure 4. Ionic conductivity as a function of temperature for all ionic liquids.

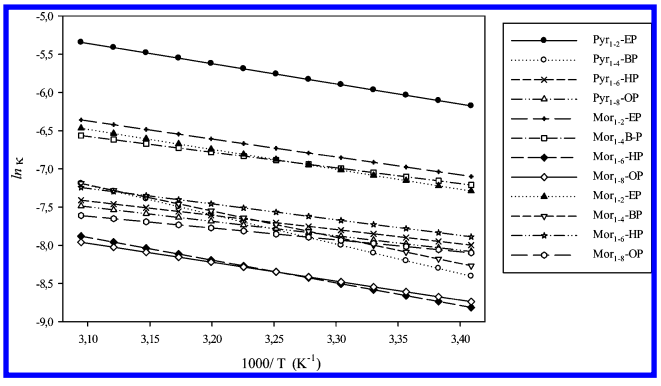

Figure 5. Plot of ln κ against 1000/T for the all ILs at the temperature range 293.15 to 323.15 K.

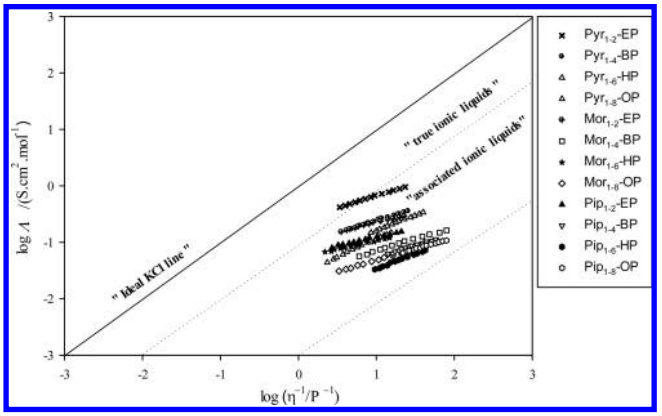

Figure 6. Walden plots for cyclic ammonium-based ionic liquids with alkylphosphite substituents, where Λ is the equivalent conductivity and η^{-1} is the fluidity. The ideal line runs from corner to corner of a square diagram is generated from data obtained in aqueous 0.01 M KCl solution.

expected due to considerably higher viscosity values. This means that a positive or negative discrepancy from the Walden product ($\Lambda\eta$) of dilute KCl solutions in which the ions are completely dissociated is a strong indication of the significant degree of ion dissociation.[44,48] Here, the Walden products for the 12 alkylphosphite-substituted ILs are apparently less than that of KCl solution, indicating a significant fraction of ion association and ion decoupling (namely, different ion mobility between cation and anion) in the ILs. Moreover, the α values are less than one ($0.30 < \alpha < 0.65$), which allows to conclude that the conductivity of ILs is not strictly controlled by the viscosity variations. This confirms the assumption that these ionic liquids are strongly associated.

3.2.3. Electrochemical Stability of RTILs. The potential window is the one of most important properties in electrochemical applications of RTILs. The resistance of the anion and cation to the oxidation and the reduction allows one to determines the extent of the electrochemical window. The potential window of the ILs was determinated by voltammetric methods. A linear sweep voltammogram of a vitrous carbon disk electrode in each cyclic ammonium alkylphosphite family at 298.15 K is shown, respectively, in Figure 7 (pyrroliddium cations), Figure 8 (morpholinium cations), and Figure 9 (piperidinium cations). The cathodic, anodic limiting potential, and electrochemical windows of the ILs determined from their linear sweep voltammograms are listed in Table 4. The potential window is defined as the potential range where the limiting current density is equal to 0.1 mA·cm^{-2}. The potential window (ΔE) ranges for the studied RTILs are from 2.99 to 4.77 V/SHE. These values are higher to those previously found for of a series of thioether-functionalized ionic liquids based on dialkylphosphate (ΔE approximately 2 V)[49] and slightly lower than usual aprotic ILs (ΔE approximately 4.5 V to 5 V).[50] An interesting phenomenon was found for the three cyclic ammonium families which show that both oxidative voltage

dx.doi.org/10.1021/je4007053 | J. Chem. Eng. Data 2014, 59, 1193−1201

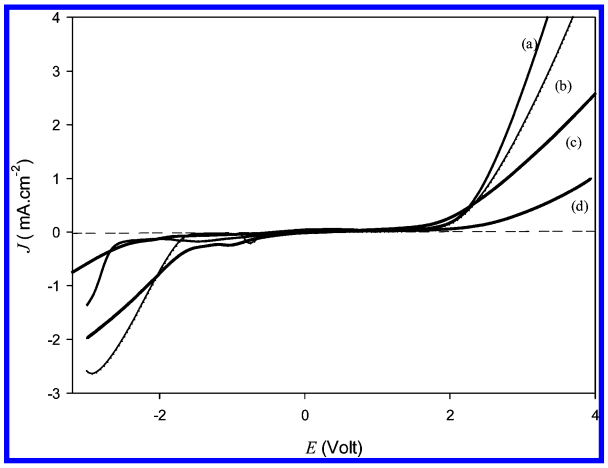

Figure 7. Linear voltammograms recorded at vitreous carbon electrode versus the $Ag/AgCl_{sat}$,KCl_{sat}(IL) reference electrode of Pyr_{1-2}-EP (a); Pyr_{1-4}-BP (b); Pyr_{1-6}-HP (c); and Pyr_{1-8}-OP (d) at a scan rate of 100 mV·s^{-1} (d). Potential was calibrated using the redox potential of ferrocene/ferricenium (Fc/Fc^+) redox couple measured in each ionic liquid.

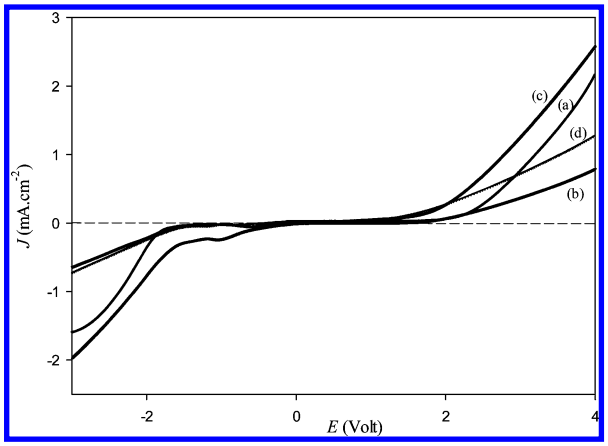

Figure 8. Linear voltammograms recorded at vitreous carbon electrode versus the $Ag/AgCl_{sat}$,KCl_{sat}(IL) reference electrode of Mor_{1-2}-EP (a); Mor_{1-4}-BP (b); Mor_{1-6}-HP (c); and Mor_{1-8}-OP (d) at a scan rate of 100 mV s^{-1}. Potential was calibrated using the redox potential of ferrocene/ferricenium (Fc/Fc^+) redox couple measured in each ionic liquid.

and reductive voltage decrease when the chain length of alkyl substitution is increasing. In ionic liquid medium, it has been shown that the oxidation of the anion and the reduction of the cation are responsible for the anodic and cathodic limits, respectively, that define the electrochemical window of RTILs.[51−53] The process of the reduction is expected to mainly involve the positively charged nitrogen in the cyclic ammonium (pyrrolidinium, piperidiniuim, and morpholinium). As indicated by Table 3, the order of electrochemical stability of the ionic liquid cation is $[Pyr_{1\text{-}n}^+] > [Pip_{1\text{-}n}^+] > [Mor_{1\text{-}n}^+]$. The cyclic pyrrolidinium seems more resistant to reduction than a piperidinium and morpholinium cations. The anodic stability is mainly determined by the potential at which the oxidation of the alkyl-phosphonate anions takes place. The anion stability toward oxidation follows the order: $[EP^-] > [BP^-] > [HP^-] > [OP^-]$. The electrochemical stabilities of the studied cyclic ammonium-based ILs were affected by the alkyl substitution. This result is interpreted in terms of electrostatic interactions between the cations and anion of ILs. The electrostatic force

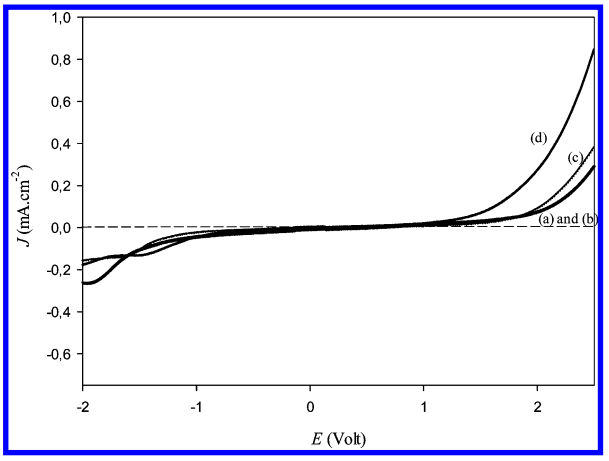

Figure 9. Linear voltammograms recorded at vitreous carbon electrode versus the $Ag/AgCl_{sat}$,KCl_{sat}(IL) reference electrode of Pip_{1-2}-EP (a); Pip_{1-4}-BP (b); Pip_{1-6}-HP (c); and Pip_{1-8}-OP (d) at a scan rate of 100 mV·s^{-1}. Potential was calibrated using the redox potential of ferrocene/ferricenium (Fc/Fc^+) redox couple measured in each ionic liquid.

Table 4. Electrochemical Windows of Selected Ionic Liquids at 298.15 K[a]

ionic liquid	E_c/vs (Fc/Fc^+)/V	E_a/vs (Fc/Fc^+)/V	electrochemical window (ΔE) /V
Pyr_{1-2}-EP	−2.54	+2.23	4.77
Pyr_{1-4}-BP	−1.87	+2.20	4.07
Pyr_{1-6}-HP	−1.69	+2.17	3.86
Pyr_{1-8}-OP	−1.33	+1.80	3.13
Mor_{1-2}-EP	−1.75	+2.26	4.01
Mor_{1-4}-BP	−1.51	+1.89	3.40
Mor_{1-6}-HP	−1.41	+1.83	3.24
Mor_{1-8}-OP	−1.40	+1.59	2.99
Pip_{1-2}-EP	−2.37	+2.11	4.48
Pip_{1-4}-BP	−1.34	+2.17	3.51
Pip_{1-6}-HP	−1.30	+2.16	3.46
Pip_{1-8}-OP	−1.17	+2.09	3.26

[a]Standard uncertainties u are $u(T)$ = 0.01 K, $u(E)$ = 0.01·E, and $u(\Delta E)$ = 0.01·ΔE.

between the cyclic ammonium and the alkyl-phosphonate is considerably weakened by the increase in the alkyl chain length of both cations and anions. Therefore, increasing the number of carbon atoms in the side chain of the cation and anion decreases the electrochemical window of ILs.

5. CONCLUSION

A novel family of RTILs based on cyclic ammonium cations with alkylphosphate anions was synthesized and characterized. The ILs density are slightly lower than densities of usual ILs. However, the isobaric thermal expansion coefficient values are of the same order of magnitude compared to common ILs. These ionic liquids exhibit a relatively high viscosity and a lower conductivity. This may be due to the strong van der Waals interactions through the increase in the alkyl side chain length of anions and cations. The Walden rule analysis showed that ionic conductivity is not controlled by viscosity variations and therefore, these ILs are strongly associated. The dynamic viscosity and conductivity dependences on the temperature has been fitted to the Arrhenius law with high precision. The potential window ranges are wide and ranging from 3 V/SHE

dx.doi.org/10.1021/je4007053 | J. Chem. Eng. Data 2014, 59, 1193−1201

to 4.77 V/SHE. The electrochemical stabilities of the studied ILs were influenced by the alkyl substitution and the electrostatic interactions between the cations and anion of ILs. All physico-chemical properties obtained in this work indicate that these new ionic liquids could be applied to electrochemical synthesis, extraction of metal cations, and preparation of nanoparticles, given their structuring character and complexing capacity of the alkyl phosphonate. Our current investigations are focused on the electrochemical synthesis of some copolymers, the extraction of some metal cations, and the preparation of AuNP and AgNP nanoparticles in these structuring media

■ ASSOCIATED CONTENT

Supporting Information

Table S_1, experimental density of all pyrrolidinium, morpholinium and piperidinium based ionic liquids at all studied temperatures and at 0.1 MPa; Table S_2, dynamic viscosity of all ionic liquids at temperatures ranging from 293.15 K to 323.15 K and at 0.1 MPa; Table S_3, ionic conductivity of all ionic liquids at temperatures ranging from 293.15 K to 323.15 K and at 0.1 MPa. This material is available free of charge via the Internet at http://pubs.acs.org.

■ AUTHOR INFORMATION

Corresponding Author

*E-mail: ramzi.zarrougui@gmail.com.

Notes

The authors declare no competing financial interest.

■ REFERENCES

(1) Zhang, S.; Lu, X.; Zhou, Q.; Li, X.; Zhang, X.; Li, S. *Ionic Liquids: Physicochemical Properties*; Elsevier: Amsterdam, The Netherlands, 2009.
(2) Angell, C. A.; Xu, W.; Yoshizawa-Fujita, M.; Hayashi, A.; Belieres, J.-P.; Lucas, P.; Videa, M.; Zhao, Z.-F.; Ueno, K.; Ansari, Y.; Thomson, J.; Gervasio, D. Physical Chemistry of Ionic Liquids: Inorganic and Organic as Well as Protic and Aprotic. In *Electrochemical Aspects of Ionic Liquids*, 2nd ed.; Ohno, H., Ed.; John Wiley & Sons, Inc.: Hoboken, NJ, 2011; pp 5−31.
(3) Koel, M., Ed. *Ionic Liquids in Chemical Analysis*; CRC Press: Boca Raton, FL, 2009.
(4) Acree, W. E.; Grubbs, L. M. Analytical Applications of Ionic Liquids. In *Encyclopedia of Analytical Chemistry*; John Wiley & Sons, Ltd.: Chichester, U.K., 2012
(5) Bockris, J. O.M.; Reddy, A. K. N. *Modern Electrochemistry*; Plenum Press: New York, 1998.
(6) Welton, T. *Chem. Rev.* **1999**, *99*, 2071−2083.
(7) Fuller, J.; Carlin, R. T.; Osteryoung, R. A. *J. Electrochem. Soc.* **1997**, *144*, 3881−3886.
(8) Earle, M. J.; McCormac, P. B.; Seddon, K. R. *Green Chem.* **1999**, *1*, 23−25.
(9) Lee, C. W. *Tetrahedron Lett.* **1999**, *40*, 2461−2464.
(10) Holbrey, J. D.; Seddon, K. R. *Clean Prod. Proc.* **1999**, *1*, 223−236.
(11) Zhang, B.; Yan, N. *Catalysts* **2013**, *3*, 543−562.
(12) Quinn, B. M.; Ding, Z.; Moulton, R.; Bard, A. J. *Langmuir* **2002**, *5*, 1734−1742.
(13) Hsiu, S. I.; Tai, C. C.; Sun, I. W. *Electrochim. Acta* **2006**, *51*, 2607.
(14) Villar-Garcia, I. J.; Abebe, A.; Chebude, Y. *Inorg. Chem. Commun.* **2012**, *19*, 1−3.
(15) Pandey, G. P.; Hashmi, S. A. J. *Mater. Chem. A* **2013**, *1*, 3372−3378.
(16) Reiter, J.; Paillard, E.; Grande, L.; Winter, M.; Passerini, S. *Electrochim. Acta* **2013**, *91*, 101−107.
(17) Ignat'ev, N. V.; Barthen, P.; Kucheryna, A.; Willner, H.; Sartori, P. *Molecules* **2012**, *17*, 5319−5338.
(18) Tang, S.; Bakerband, G. A.; Zhao, H. *Chem. Soc. Rev.* **2012**, *41*, 4030−4066.
(19) Muhammad, N.; Man, Z.; Ziyada, A. K.; Bustam, M. A.; Abdul Mutalib, M. I.; Wilfred, C. D.; Rafiq, S.; Tan, I. M. *J. Chem. Eng. Data* **2012**, *57*, 737−743.
(20) Ganeshpure, P. A.; George, G.; Das, J. *J. Mol. Catal. A: Chem.* **2008**, *279*, 182−186.
(21) Zhang, S.; Sun, N.; He, X.; Lu, X.; Zhang, X. *J. Phys. Chem. Ref. Data* **2006**, *35*, 1475−1518.
(22) Greaves, T. L.; Drummond, C. J. *Chem. Rev.* **2008**, *108*, 206−237.
(23) Kenneth, R. S.; Stark, A.; Torres, M.-J. *Pure Appl. Chem.* **2000**, *72*, 2275−2287.
(24) Yuehui, Z.; Robertson, A. J.; Hillhouse, J. H.; Douglas, B. *Phosphonium and imidazolium salts and methods of their preparation.* , U.S. Patent Application 20060264645, November 23, 2006.
(25) Gonzalez, B.; Gomez, E.; Domenguez, A.; Vilas, M.; Tojo, E. *J. Chem. Eng. Data* **2011**, *56*, 14−20.
(26) Nguyen, H.-P.; Baboulene, M. *Alkyl H-phosphonates of N,N′-dialkylimidazoliums and of quaternary ammoniums and uses thereof*. U.S. Patent Application 20100121075, May 13, 2010.
(27) Mitsuru, A.; Yukinobu, F.; Ohno, H. *Green Chem.* **2010**, *12*, 1274−1280.
(28) Fukaya, Y.; Hayashi, K.; Wada, M. *Green Chem.* **2008**, *10*, 44−46.
(29) Esser, J.; Wasserscheid, P.; Jess, A. *Green Chem.* **2004**, *6*, 316−322.
(30) Meinsdersma, G. W.; Podt, A. J. G.; De Haan, A. B. S. In *Ionic Liquids III: Fundamentals, Progress, Challenges, and Opportunities*; Rogers, R. D, Seddon, K., Eds.; ACS Symposium Series 901−902; American Chemical Society: Washington, DC, 2005.
(31) Meinsdersma, G. W.; Podt, A. J. G.; De Haan, A. B. S. *Fluid Phase Equilib.* **2006**, *247*, 158−168.
(32) Troev, K. D. *Chemistry and Application of H-Phosphonates*; Elsevier Science: Amsterdam, The Netherlands, 2006.
(33) Hall, H. K. *J. Am. Chem. Soc.* **1957**, *79*, 5441−5444.
(34) Sharma, G. P.; Sobti, R. C.; Sahi, K. *Natl. Acad. Sci. Lett.* **1980**, *3*, 187−188.
(35) Wu, Zi-Yi.; Su, S.-G.; Gung, S.-T.; Lin, M.-W.; Lin, Y.-C.; Lai, C.-A.; Sun, I.-W. *Electrochim. Acta* **2010**, *55*, 4475−4482.
(36) Almeida, H. F. D.; Passos, H.; Lopes-da-Silva, J. A.; Fernandes, A. M.; Freire, M. G.; Coutinho, J. A. P. *J. Chem. Eng. Data* **2012**, *57*, 3005−3013.
(37) Krolikowska, M.; Hofman, T. *Thermochim. Acta* **2012**, *530*, 1−6.
(38) Catarina, M. S. S.; Neves, P. J.; Carvalho, M.; Freire, G.; Coutinho, J. A.P. *J. Chem. Thermodyn.* **2011**, *43*, 948−957.
(39) Dzyuba, S. V.; Bartsch, R. A. *ChemPhysChem* **2002**, *6*, 161−166.
(40) Tokuda, H.; Hayamizu, K.; Ishii, K.; Susan, M. A. H.; Watanabe, M. J. *Phys. Chem. B* **2005**, *109*, 6103−6110.
(41) Cai, Y.; Li, Z.; Zhang, H.; Fang, Y.; Fan, X.; Liu, J. *Electrochim. Acta* **2010**, *55*, 4728−4733.
(42) Bonhote, P.; Dias, A. P.; Papageorgiou, N.; Kalyanasundaram, K.; Gratzel, M. *Inorg. Chem.* **1996**, *35*, 1168−1178.
(43) Zarrougui, R.; Dhahbi, M.; Lemordant, D. *J. Solution Chem.* **2010**, *39*, 921−942.
(44) Brigouleix, C.; Anouti, M.; Jacquemin, J.; Caillon-Caravanier, M.; Galiano, H.; Lemordant, D. *J. Phys. Chem. B* **2010**, *114*, 1757−1766.
(45) Anouti, M.; Caillon-Caravanier, M.; Le Floch, C.; Lemordant, D. *J. Phys. Chem. B* **2008**, *112*, 9406−9411.
(46) Xu, W.; Angell, C. A. *Science* **2003**, *302*, 422.
(47) Ficke, L. E.; Novak, R. R.; Brennecke, J. F. *J. Chem. Eng. Data* **2010**, *55*, 4946−4950.
(48) Xu, W.; Cooper, E. I.; Angell, C. A. *J. Phys. Chem. B* **2003**, *107*, 6170−6178.

(49) Torriero, A. A. J.; Siriwardana, A. I.; Bond, A. M.; Burgar, I. M.; Dunlop, N. F.; Deacon, G. B.; MacFarlane, D. R. *J. Phys. Chem. B* **2009**, *113*, 11222−11231.
(50) MacFarlane, D. R.; Meakin, P.; Sun, J.; Amini, N.; Forsyth, M. *J. Phys. Chem. B* **1999**, *103*, 4164−4170.
(51) Suarez, P. A. Z.; Consorti, C. S.; de Souza, R. F.; Dupont, J.; Gonçalves, R. S. *J. Braz. Chem. Soc.* **2002**, *13*, 106−109.
(52) Suarez, P. A. Z.; Selbach, V. M.; Dullius, J. E. L.; Einloft, S.; Piatnicki, C. M.; Azambuja, D. S.; de Souza, R. F.; Dupont, J. *Electrochim. Acta* **1997**, *42*, 2533−2535.
(53) Zein El Abedin, S.; Borissenko, N.; Endres, F. *Electrochem. Commun.* **2004**, *6*, 510−514.